Polymer Chemistry

Accepted Manuscript

ROYAL SOCIETY OF CHEMISTRY

www.rsc.org/polymers

Cite this: DOI: 10.1039/c0xx00000x

www.rsc.org/xxxxxx

ARTICLE TYPE

Thermoresponsive Poly (*N*-Vinylcaprolactam-co-Sulfobetaine Methacrylate) Zwitterionic Hydrogel Exhibiting Switchable Anti-Biofouling and Cytocompatibility

Boguang Yang,[a] Changyong Wang, [b]Yabin Zhang,[a] Lei Ye,[a]Yufeng Qian,[c]Yao Shu,[b] Jinmei Wang,[a]Junjie Li*[ab] and Fanglian Yao*[ab]

Received (in XXX, XXX) XthXXXXXXXXX 20XX, Accepted Xth XXXXXXXXX 20XX
DOI: 10.1039/b000000x

Nonspecific protein adsorption adversely affects the application of thermoresponsive polymer in biomedical field. To overcome this disadvantage, we used thermoresponsive *N*-vinylcaprolactam (VCL) and anti-biofouling zwitterionic sulfobetaine methacrylate (SBMA) monomers with various VCL/SBMA ratios, and synthesized the (P (VCL-co-SBMA)) copolymers via free radical solution polymerization. The P (VCL-co-SBMA) copolymers exhibit both lower critical solution temperature (LCST) and upper critical solution temperature (UCST) in aqueous solutions. Moreover, both the UCST and LCST of the copolymer shift to higher temperatures with the increase of PSBMA segments, and they shift to lower temperatures with the increase of salt concentrations in the solution. Based on these results, P (VCL-co-SBMA) hydrogels were prepared using *N, N'*-methylenebisacrylamide (MBAA) as the cross-linker. Compared with the PVCL hydrogel, the P (VCL-co-SBMA) hydrogels exhibit better mechanical property. Notably, the P (VCL-co-SBMA) hydrogel retained the temperature-sensitivity of PVCL, and it can be modulated by varying PVCL/PSBMA segments ratios. In addition, all hydrogels exhibit good cytocompatibility. More importantly, the protein adsorption and cell adhesion on the hydrogel can be controlled by the temperature. The nonspecific protein adsorption was effectively suppressed at physiological temperature. The switchable anti-biofouling nature of P (VCL-co-SBMA) hydrogel along with their temperature sensitivity can be potentially used in drug, cell or enzymes delivery.

1. Introduction

Thermoresponsive polymer, which undergo a reversible phase transition at a specific temperature,[1] have been widely applied to prepare hydrogel based carrier to deliver drug,[2, 3] enzymes or cells.[4, 5] These biomedical devices contact with biological microenvironment when they are injected or implanted *in vivo*.[6] During this process, it is inevitable that biofouling from some nonspecific biomolecules can occur on the surface of these devices, which may lead to undesirable consequences including reduction in the efficacy/sensitivity of carriers,[7] thrombosis,[8] and microbial infections.[9] Unfortunately, most of the existing thermoresponsive hydrogels are less efficient in anti-biofouling activity against protein adsorption and cell attachment. Therefore, it is necessary to prepare thermoresponsive hydrogels possessing anti-biofouling properties.[10]

Poly (*N*-isopropylacrylamide) (PNIPAAm) is one of the well-known member of the temperature sensitive polymer family, as it undergoes a hydrophilic-hydrophobic transition in water at lower critical solution temperature (LCST) (ca. 32°C), which falls between room temperature and physiological temperature.[11, 12] However, the acrylamide moiety is prone to hydrolysis in acidic conditions to release potentially toxic small amine molecules from the main polymer chain, causing unwanted side effects during long-term biomedical applications.[13] Recently, poly (*N*-vinylcaprolactam) (PVCL) emerged as an alternative thermoresponsive polymer. Similar to PNIPAAm, the PVCL undergoes a miscible to immiscible phase transition at LCST (31-34°C).[14] Nevertheless, PVCL is very stable against hydrolysis[13] and of hydrolysis of PVCL does not result in toxic amine compounds. In addition, PVCL has been shown to be biocompatible. Henna V et al.,[15] reported that the PVCL is well tolerated by cells at all concentrations (0.1-10.0 mg/ml), while the PNIPAAm showed a clear cytotoxicity at similar concentrations. Unfortunately, these PVCL based thermosensitive hydrogels display only a moderate wettability, weak mechanical properties and low anti-biofouling. Thus, efforts are under way to improve the anti-biofouling and mechanical properties of PVCL based hydrogel.

Table 1 Preparation parameters and characteristic data of P (VCL-co-SBMA) copolymers

Sample	Monomer Molar Feed Ratio		SBMA Molar Ratio in Copolymer (%)	Yield (%)	M_n (g/mol)	M_w/M_n
	VCL (%)	SBMA (%)				
PVCL	100	0	0	65.2		
P(VCL-co-SBMA)$_1$	88.9	11.1	23.6	69.7	23055	1.478
P(VCL-co-SBMA)$_2$	66.9	33.1	44.1	70.1	50615	1.319
P(VCL-co-SBMA)$_3$	46.2	53.8	56.8	72.1	59454	1.682
PSBMA	0	100	100	94.3	393728	1.327

Zwitterionic polysulfobetaine methacrylate (PSBMA) with a methacrylate main chain and a pendant group consisting of an analogue of the taurinebetaine ($CH_2CH_2N^+(CH_3)_2CH_2CH_2CH_2SO_3^-$) has been reported to be highly resistant to undesirable protein adsorption due to its high hydrophilicity.[17, 18] Unlike thermoresponsive polymer with LCST, PSBMA exhibits a sharp phase transition at an upper critical solution temperature (UCST) in aqueous solution, which is attributed to the charge-charge or dipole-dipole interactions among the zwitterionic sulfobetaine groups.[19, 20] As such, UCST can be modulated via adjusting the solvent polarities,[21, 22] ionic strength[23, 24] and copolymerization with other kinds of monomer.[20, 25, 26] In addition, PSBMA have recently been shown to have excellent biocompatibility and potential application in clinically relevant implant models.[27] Synthesizing PSBMA based biomaterials has been emerging as an active research area. Li et al.,[28] immobilized the PSBMA polymer on the silicone-g-P (PEGDMA) substrate via thiol-ene click reaction, and it leads to the increase of antifouling efficacy. Our previous work[29] also reported a new class of copolymers hydrogel prepared from the combination of the PSBMA and starch, exhibiting good anti-biofouling efficiency and biocompatibility. Recently, thermoresponsive polymer containing zwitterionic sulfobetaine groups have received growing attention.[30] Shen AQ et al,[31] synthesized copolymers poly (NIPAAm-co-SBMA) via random copolymerization. Zhang et al[32] synthesized thermoresponsive zwitterionic ABC-type triblock copolymers by atom transfer radical polymerization. The combination of LCST with UCST in these polymers shows an intriguing temperature-induced phase transition behaviors in aqueous solution,[33] non-biofouling and thermosensitive features, which have shown great advantages for biological applications *in vivo*.

In this work, we synthesized the P (VCL-co-SBMA) random copolymer with different ratios of VCL/SBMA via homogenous reaction in DMSO/water mixed solvent using redox initiating system. The phase transition temperatures including LCST and UCST of P (VCL-co-SBMA) in aqueous solution are discussed in detail. In addition, nonionic PVCL hydrogel, zwitterionic PSBMA hydrogel, and P (VCL-co-SBMA) copolymer hydrogels were prepared using *N, N'*-methylene bisacrylamide (MBAA) as the cross-linker. The temperature/ion sensitive properties, hydrophilicity and mechanical strength of prepared hydrogels were investigated. In addition, we evaluated the protein resistance of these hydrogels at different temperatures. Based on these results, the cytocompatibility, cell adhesion and detachment behavior on the P (VCL-co-SBMA) hydrogel surface, using human umbilical vein endothelial cells (HUVECs) as the model cell, were investigated at different temperatures.

2. Experimental Section

2.1 Materials

N-vinylcaprolactam (VCL, 98 %), ammonium persulfate (APS, 99%), tetramethylethylenediamie (TEMED, 99%), 3-[2-(methacryloyloxy) ethyl] (dimethyl) -ammonio] - 1-propanesulfonate (SBMA, 98%) and *N, N'*-methylenebisacrylamide (MBAA, 99%) were obtained from Sigma-Aldrich Chemical Company. All other reagents were analytical grade without further purification.

2.2 Synthesis and characterization of P (VCL-co-SBMA) copolymer

PVCL, PSBMA and P (VCL-co-SBMA) random copolymer were synthesized via free radical solution polymerization. In brief, 1.2 g VCL/SBMA with different molar ratios (Table 1) were dissolved in 15 ml DMSO/water (1:5, v/v) mixtures, and nitrogen was bubbled into the solution for 30 min to remove oxygen. Then, 23.6 mg APS and 20 µl of TEMED were rapidly added into this mixture. The reaction was carried out at 30°C under nitrogen atmosphere for 48 h. The product was dialyzed (MWCO=3500 Da) against distilled water for 3 days at room temperature to remove the unreacted reagents and impurities. Furthermore, the mixture solution was lyophilized and the PVCL, PSBMA and P(VCL-co-SBMA)$_{1-3}$ copolymer with different ratios of VCL/SBMA were obtained. The detail reaction parameters and yields were listed in Table 1.

The chemical character of PVCL, PSBMA and P (VCL-co-SBMA) was determined by ^{1}H NMR (Bruker DMX-400 spectrometer) using D_2O/NaCl as the solvent. Molecular weight and polydispersity index of these polymers were determined using gel permeation chromatography (GPC) by a Viscotek TDA305 equipped with triple detections. $NaNO_3$ aqueous solution (0.1 M, pH 7.4) was used as eluent, which is at a flow rate of 0.5 ml/min. For P (VCL-co-SBMA) copolymers and PSBMA homopolymer, the instrument constants were calibrated by monodisperse PEG (99k) standards. All measurements were performed at 30°C.

2.3 Determination of LCST and UCST of the (co)polymers

The phase transition temperatures (UCST and/or LCST) of the polymers in aqueous solutions were determined by reading the hydrodynamic diameter (D_h) using Nano Sizer Measurement (Malven, UK) based on the dynamic laser light scattering principle (DLS). Briefly, 1 ml of PVCL, PSBMA or P (VCL-co-SBMA) solution (5 wt%) was first cooled from 30°C to 0°C and then gradually heated from 0 to 80°C, and the D_h was record for

every 1°C increment of each sample after a 10 min thermal equilibration.[19] The UCST and LCST were defined as the temperature where the maximum slope for the D_h versus temperature curve occurs. In addition, the LCST and UCST of copolymer in NaCl solution with different concentration (0.01-1.5 M) are also measured.

2.4 Preparation of P (VCL-co-SBMA) hydrogels

Briefly, 1.20 g of VCL/SBMA monomer mixture with different molar ratio (cf. Table S1) was dissolved in 6 ml DMSO/H_2O mixture in a plastic tube. Then the cross-linking agent (*N, N'*-methylenebis (acrylamide), MBAA) of weight ratio 8 % relative to monomer mixture, were added into the solution and the reactive system were kept under nitrogen atmosphere to remove oxygen. After 15 min, 50 µl of APS aqueous solution (0.288 g/ml) and 11 µl of TEMED were rapidly added. The polymerization reaction was allowed to continue at 30°C for 24 h. Next, cross-linked hydrogel were taken out and extracted with water/ethanol for 24 h in a Soxhlet Extractor to remove the residual monomer and cross-linker. Finally, the hydrogel were immersed in deionized (DI) water to remove the DMSO and other impurities.

2.5 Physical and chemical properties of hydrogels

2.5.1 Hydrophilicity

The static water contact angles were measured using a goniometer (Ramé-Hart Instrument Co., Netcong, NJ) to investigate the hydrophilicity of the dry hydrogel. The dry hydrogel was positioned on top of the measure stage, and a drop of DI water was dropped on the sample. The sessile drop images of DI water on the sample were recorded using a Diamond VC500 one-touch video capture system (Diamond Multimedia, Chatsworth, CA) while the associated elapsed time was manually recorded. Meanwhile, the contact angle was measured using Image J software (National Institutes of Health, Bethesda, MD).

2.5.2 Swelling ratio

The gravimetric method was used to evaluate the swelling ratios of hydrogel. Briefly, dry PVCL, PSBMA and P(VCL-co-SBMA) hydrogel were weighed (W_d, ca. 10 mg) and immersed in 2 ml DI water at a specific temperature (4, 25, 37 or 60°C) for 48 h. The samples were carefully removed from the water and wiped with a moisture filter paper to remove the excess water, then the swollen hydrogels were weighed (W_w). The equilibrium swelling ratio (ESR) at different temperature is calculated using equation (1). The reversible swelling behaviors of hydrogel were measured at temperatures that alternated between 4°C and 37°C.

$$ESR = (W_w - W_d) / W_d \qquad (1)$$

In addition, the swelling behaviors of P (VCL-co-SBMA) hydrogels in various concentrations (0, 0.5, 1.0, 1.5, 2.0, 2.5 and 3.0 M) of NaCl aqueous solutions at 37°C were also measured using the same method. Similarly, the reversible swelling ratio was also measured in NaCl solution at concentration between 0 and 2.5 M.

2.5.3 Mechanical properties

The uniaxial compression tests of hydrogels were measured using a tensile-compressive tester (Tensilon RTC-1310A, Orientec Co.) with a 100 N load cell. All hydrogel samples were column with a 15 mm diameter and 10 mm high. A crosshead speed of 0.1 mm/min was used. The fracture stress and the fracture strain were determined as the nominal stress and the nominal strain at the failure point. Compression modulus was also determined by the equation (2) as the slope at the 0-20 % strain range from the stress-strain curve, where E is the modulus, σ is the stress, and ε denotes the strain.

$$E = \sigma/\varepsilon \qquad (2)$$

2.6 Protein adsorption

Direct enzyme-linked immunosorbent assay (ELISA) was used to measure immunoglobulin G (IgG) adsorption onto the various hydrogels at different temperatures. PVCL, PSBMA and P (VCL-co-SBMA) hydrogels were punched into discs with a diameter of 5.0 mm and a thickness of 2.0 mm. The wet hydrogel discs were immersed in 1 ml PBS (pH=7.4) at 4, 37 and 60 °C for 24 h to achieve the equilibrium swelling. Then, the PBS was removed and the hydrogels discs were incubated in 400 µl IgG-HRP PBS solution (1 µg/ml) at 4, 37 and 60°C for 60 min, respectively. After rinsing with PBS five times, the samples were transferred to new container and immersed in 500 µl of 0.1 M phosphate-citrate buffer containing 1 mg/ml o-phenylenediamine (OPD) and 0.03 % hydrogen peroxide, incubating for 15 min at 37°C for the colour development. Finally, the reaction was stopped by adding 500 µl sulfuric acid solutions (1.0 M). The absorbance at 492 nm was measured by a Tecan Infinite M200 microplate reader (Switzerland). The positive control for this experiment was the ELISA plate, and the negative control was the phosphate-citrate buffer containing 1 mg/ml OPD and 0.03 % hydrogen peroxide without IgG-HRP during the ELISA test.

2.7 Cell experiment

For the experiments of cell adhesion and proliferation, Human Umbilical Vein Endothelial cells (HUVECs) were seeded on the surface of hydrogels. Culture medium (1 ml) containing 2×10^4 cells were added to 24-well tissue culture plate covered by PVCL, PSBMA and P (VCL-co-SBMA) hydrogel discs with a diameter of 10.0 mm and a thickness of 2.0 mm. The cells were allowed to attach on the surface of hydrogel at 37°C incubator with 5% CO_2 for 1, 4, and 7 days. The cells morphology was observed using fluorescence microscope after stained by acridine orange and propidium iodide (AO/PI). Meanwhile, the cell viability was determined by MTT assay. Briefly, 50 µl MTT (Sigma, 5 mg/ml) was added to each well and incubated at 37°C, 5% CO_2 for 4 h. After removing the medium and 500 µl DMSO was added in each well, 100 µl solution of each sample was transferred to a 96-well plate. The optical density (OD) was determined at 492 nm.

Temperature-assisted cell detachment was also evaluated using fluorescent staining. Briefly, the cell were stained using AO/PI after cultured for 5 days, and then placed at 4 and 25°C for 30, 60, and 120 min, respectively. The HUVECs adhered on the surface of hydrogel discs was observed using a CCD camera mounted on Olympus BX51.

3. Results and Discussion

3.1 Synthesis of P (VCL-co-SBMA) copolymers

Figure 1A shows the route for synthesis of P (VCL-co-SBMA) random copolymers via free radical solution polymerization. The polymerization reactions with different monomer feeding ratios of VCL/SBMA (Table 1) were carried out in DMSO/H_2O using APS/TEMED as the initiator. ^{1}H NMR was then used to confirm the formation of P (VCL-co-SBMA) copolymers. As shown in Figure 1B, ^{1}H NMR signal corresponding to -CH_2- proton of PVCL appears as a broad peak from 1.1 to 1.9 ppm, whereas the signal corresponding to methylene protons (2H, -N^+CH_2-) and methyl protons (6H, -$N^+(CH_3)_2$-) of the PSBMA appears at 3.6 ppm and 3.1 ppm, respectively. The presence of proton signals of PVCL and PSBMA segments confirm the formation of P (VCL-co-SBMA).

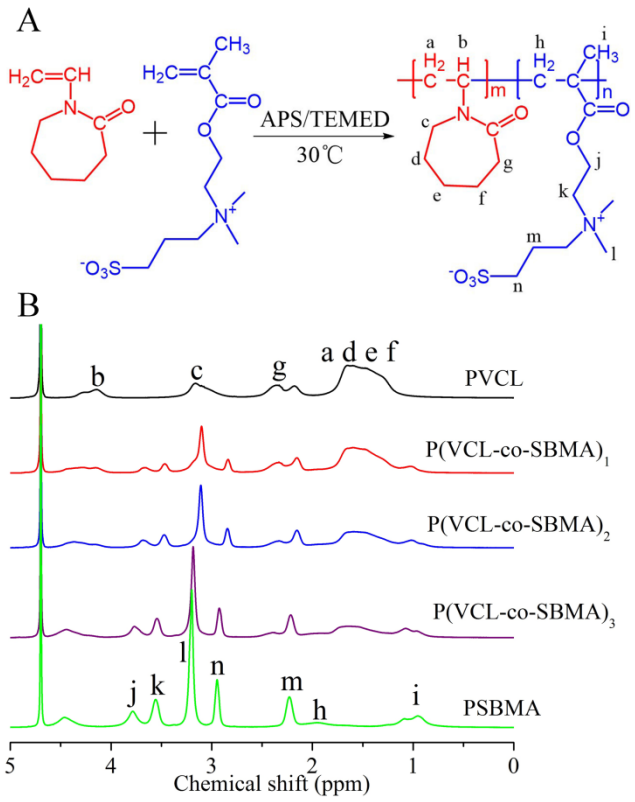

Figure 1. (A) Outline of the synthesis of the P (VCL-co-SBMA) copolymers and (B) ^{1}H NMR spectra of the polymers

The molecular weight (M_w) and polydispersity index (M_w/M_n) of the (co)polymers were estimated by GPC. Typical GPC traces of the copolymers reveal a monomodal and symmetric elution peak (Figure S1), indicating that there is no homopolymer formed during the copolymerization reaction. Moreover, the molecular weight distributions of all samples fall into a moderate range (i.e. M_w/M_n=1.3-1.7) (cf. Table 1). The M_n of P (VCL-co-SBMA) copolymers increases from 2.3 kDa to 5.9 kDa with the increase of SBMA monomers in the reaction system. The molar ratio of SBMA and VCL in the P(VCL-co-SBMA) copolymer was determined by comparing integrated area of the peak at 2.9 ppm (the protons at -$CH_2SO_3^-$ of PSBMA segment) to that of peak (g) at 2.5 ppm (the protons at -CH_2CO- of PVCL segment). Our data suggest that the molar content of SBMA segments in copolymers can be modulated by varying the monomer feeding ratio of VCL/SBMA in the reaction. (cf. Table 1). The content of VCL in copolymer decreases with the decrease of feeding ratio of VCL/SBMA. The molar content of PVCL segments in the P(VCL-co-SBMA)$_2$ copolymers is only 55.9 mol % even though the amount of VCL monomers used in the reaction system is as high as 66.9 mol%. It appears that SBMA monomers have a higher polymerization reactivity than that of VCL monomers in the reaction system, which maybe due to the VCL's unconjugated structure[34, 35] and steric hindrance of caprolactam groups.[35]

3.2 Phase transition temperatures of P (VCL-co-SBMA)

As double stimuli-responsive copolymers, P (VCL-co-SBMA) could self-assemble into more than one type of aggregates (i.e., so-called "schizophrenic" aggregation) in aqueous solution depending on the external conditions, such as temperature and ionic strength. Figure 2A shows the hydrodynamic diameters (D_h) of P (VCL-co-SBMA) in water at different temperatures, which are used to determine the phase transition temperatures. Below 34°C, the D_h of PVCL is between 31 and 33 nm, while the D_h sharply increases to over 12000 nm when the temperature is above 34°C, indicative of the aggregation of PVCL polymer. This result suggests that the nonionic PVCL exhibits a LCST in water at 34°C. Our data is consistent with the results reported by Sun ST et al.,[36] showing that PVCL exhibits a LCST in water ranging from 30°C to 50°C, which are caused by the intra and inter molecular interactions between PVCL molecular chains. Above the LCST, the hydrophobic caprolactam rings of PVCL aggregate into collapsed coil because the hydrogen bonds between PVCL and water decreases, resulting in soluble-insoluble phase transitions.[36] In contrast, the PSBMA shows the largest D_h (ca. 6000 nm) below 38°C, while its D_h rapidly decreases to 42 nm when the temperature increased to 46°C, which indicates that PSBMA exhibits an UCST in aqueous solutions at 46°C. When temperatures below the UCST, PSBMA exists as a collapsed coil and precipitates out of the solution, due to strong mutual intra and intermolecular associations of the zwitterionic groups by electrostatic interactions.[6] When temperatures above the UCST, the thermal energy is sufficiently high to break the electrostatic attractions by ion pairings between the ammonium-cation and the sulfo-anion, and thus cause the phase transitions of aggregate-to-unimer.[20, 37]

After the incorporation of PSBMA segments to the PVCL ones, the LCSTs shift from 34°C to 36°C for P(VCL-co-SBMA)$_1$, 38°C for P(VCL-co-SBMA)$_2$ and 43°C for P(VCL-co-SBMA)$_3$ (Figure 2A). It is because the hydrophobic interactions among PVCL segments become weaker when the PSBMA segment is incorporated.[31] Interestingly, P(VCL-co-SBMA)$_2$ and P(VCL-co-SBMA)$_3$ copolymers, which have higher ratio of PSBMA segments, not only shows LCSTs, but also exhibit USCTs at 9°C and 27°C, respectively (Figure 2A). The P (VCL-co-SBMA)$_{2\text{-}3}$ copolymers only remain soluble in water at temperatures between UCST and LCST. Moreover, it should be noted that both of the LCST and UCST shift to higher temperatures as the increase of PSBMA segments in the copolymer. The phase transitions from aggregate-to-unimer-to-aggregate of "schizophrenic" copolymer

at different temperature can be explained by distinct intra and inter molecular interactions between copolymer chains (Figure 3). Both PVCL and PSBMA segments in copolymer are hydrophilic when the temperature is between UCST and LCST (Figure 3B), so that these copolymers can dissolve in water (Figure 3E). When the temperature is above LCST, the aggregates consisting of hydrophobic PVCL core and hydrophilic PSBMA outer corona are formed (Figure 3C and 3F), which is possibly driven by the dehydration of PVCL for a more favorable entropic gain of the system as a whole. Similarly, at temperatures lower than the UCST, another type of aggregates is formed with PSBMA segments as the core and well-solvated PVCL segments as the corona (Figure 3A and 3D) through the associations of the zwitterionic groups by electrostatic interactions.[20]

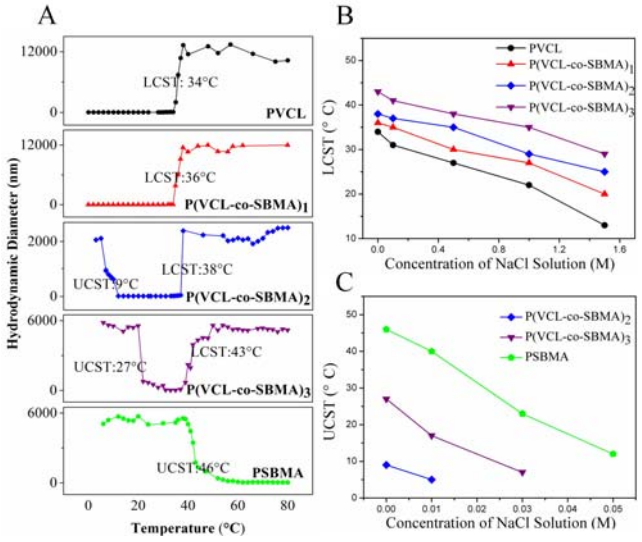

Figure 2. Phase transition behavior of P (VCL-co-SBMA) copolymers in aqueous solution (5 wt%). (A) Hydrodynamic diameter of (co)polymers in aqueous solutions at different temperatures; (B) Effect of ionic strength on LCST of the (co)polymer in NaCl solutions; (C) Effect of ionic strength on UCST of the (co)polymer in NaCl solutions with different concentrations.

Ionic strength is another key parameter to modulate the phase transition behaviors of many synthetic polymers.[20] Therefore, we then sought to examine the roles of ionic strength on the phase transitions of the prepared polymers in various concentrations of NaCl solution. As shown in Figure 2B and 2C, both of the UCST and LCST of P(VCL-co-SBMA) copolymers gradually decrease with the increase of salt concentrations. For PVCL and P(VCL-co-SBMA) with higher PVCL segments, the addition of electrolyte ions (Na^+ and Cl^-) enhances the ion-water interactions and disrupts the hydrogen-bonding of water molecules with caprolactam moieties, resulting in the decrease of LCST (Figure 2B and Figure 3I).[38, 39] For PSBMA and P(VCL-co-SBMA) with a higher PSBMA segments, there are net attractive electrostatic interactions among the polymer chains when the temperature < UCST, which causes the polymer chains to collapse and the polymer precipitates from the solution (Figure 3G and 3H).[40] Addition of ions will attenuate and even screen the electrostatic interactions among zwitterionic PSBMA segments, and promotes copolymer chains expansion and thus solubility in water, which overall causes UCST shifts to a lower temperature.[17]

3.3 Formation and characterization of P(VCL-co-SBMA) hydrogels

The P(VCL-co-SBMA) hydrogel was fabricated by free radical copolymerization of VCL and SBMA using MBAA as cross-linker, and APS/TEMED as the redox initiator (Figure 4A). The chemical structures of P(VCL-co-SBMA) hydrogels were characterized by FTIR spectroscopy (Figure 4B). All three P(VCL-co-SBMA) hydrogels show carboxyl (C=O) absorption bands of ester group in PSBMA segments at 1727 cm^{-1}. The absorption peak at 1033 cm^{-1} is assigned to symmetric stretching of the sulfonate groups in the PSBMA segments. Moreover, the adsorption intensity of these peaks increases as the increase of PSBMA segments in hydrogel. Likewise, the intensity of asymmetric stretching vibration of S=O group at 1183 cm^{-1} and C-H stretching of the $-N^+(CH_3)_2-$ group at 1487 cm^{-1} also increase with the increase content of PSBMA segments.[23] In addition, carboxyl (C=O) absorption bands at 1650cm^{-1} of amide group in PVCL segments can also be observed in FTIR spectra, and its adsorption strength decreases with the decrease of PVCL segments.

The hydrophilicity/hydrophobicity of hydrogel surfaces plays very important roles in the protein adsorption. The water contact angles of the material surfaces were used to evaluate the hydrophilicity/hydrophobicity of the copolymers. As shown in Figure 4C, the water contact angle gradually decreases from 59.88±2.81 to 45.44±1.69° with the increase of PSBMA segments (from 0% to 100%) at room temperature, indicating that the surface become more hydrophilic. In fact, PVCL can only bind water through hydrogen bonds between water molecules and amide groups,[36] while PSBMA can bond water via more interactions between water molecules and $-SO_3^-$ group or $-N^+(CH_3)_2-$ group of sulfobetaines.[10, 44]

Hydrogels with adequate mechanical strength are desirable for biomedical applications. Representative stress-strain curves of the prepared hydrogels are presented in Figure 4D. All hydrogels exhibit linear stress-strain curves at the initial stage, which corresponds to the elastic region of these hydrogels. The break strain of P(VCL-co-SBMA) hydrogel is higher than that of PVCL hydrogel, although it is less than that of PSBMA hydrogel. Consistently, the $P(VCL\text{-}co\text{-}SBMA)_3$ with a higher ratio of SBMA shows higher stress responses over the elastic region, we find that the compression modulus increases with the increase of SBMA segments (Figure 4E). The PVCL hydrogel shows the lowest mechanical strength and is very brittle, while PSBMA hydrogel displays highest mechanical strength. Meanwhile, $P(VCL\text{-}co\text{-}SBMA)_3$ hydrogels exhibit similar mechanical properties compared with PSBMA hydrogels. These features are due to complex intermolecular interactions among PSBMA segments. It could be speculated that the strong electrostatic interactions between PSBMA segments are weakened because of the steric hindrance of caprolactam moieties.[42, 43] These results indicate that the introduction of PSBMA segment can improve the mechanical properties of PVCL hydrogel.

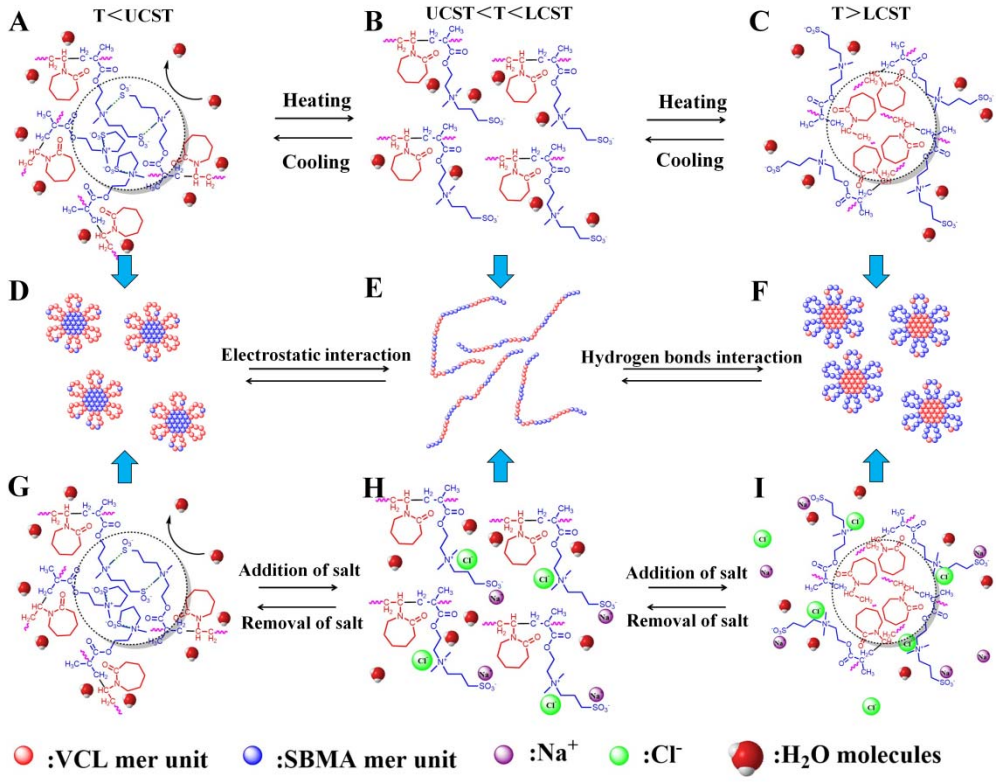

Figure 3. Schematic illustration of the temperature and ionic strength dependences of the association performance of P(VCL-co-SBMA) copolymers in aqueous solution.

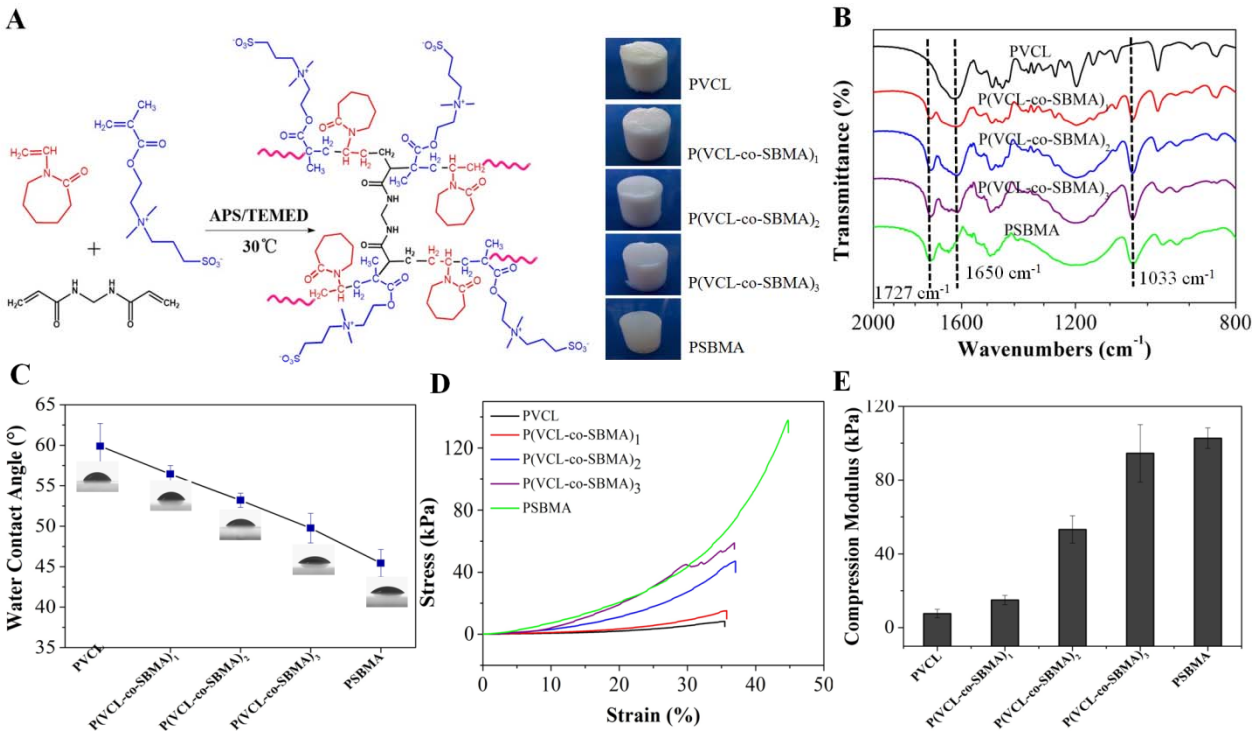

Figure 4. Characteristics of P(VCL-co-SBMA) hydrogel with different ratio of VCL/SBMA. (A) Synthesis scheme and morphology; (B) FTIR spectra; (C) Contact angles of dry hydrogel surface; (D) Compressive stress-strain curves, and (E) Compression modulus.

3.4 Temperature sensitivity of hydrogels

To investigate the temperature sensitivity of P(VCL-co-SBMA) hydrogels, we measured the equilibrium swelling ratio (ESR) of P(VCL-co-SBMA) hydrogels at different temperatures (Figure 5A). For the PVCL hydrogel, the ESR decreases from 6.99±0.62 to 3.71±0.20 when the temperature increases from 4°C to 60°C, which is due to the nonionic PVCL associations induced by hydrophobic interactions among caprolactam moieties. At temperatures lower than LCST, hydrophilic PVCL attracts water into the hydrogel network via hydrogen bond interactions. As the temperature increases, these interactions are reduced and the energized water molecules surrounding the hydrophobic PVCL chains are released from the hydrogel network,[44] leading to a reduction of ESR. In contrast, the PSBMA hydrogels exhibit reverse swelling behaviors, with a slight increase of the ESR from 2.13±0.01 to 2.88±0.03 when the temperature increases from 4 to 60°C. As the temperature increases, the intra- and inter-molecular electrostatic interactions among the zwitterionic moieties of PSBMA are attenuated, which are in turn replaced by the hydrogen bonding with water molecules.[17]

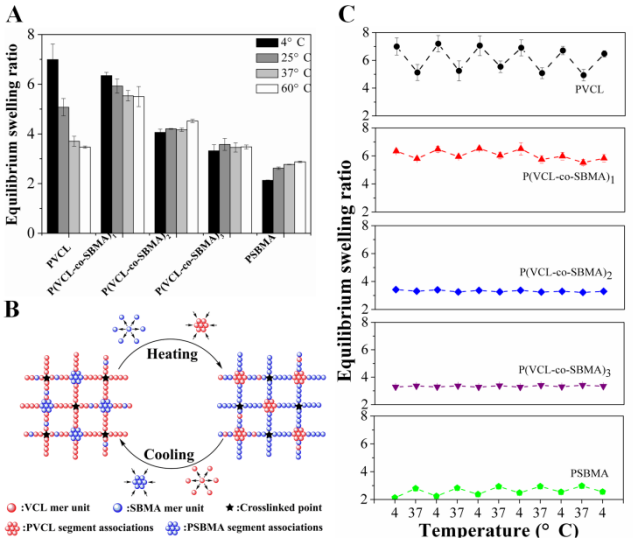

Figure 5. (A) Equilibrium swelling ratio of P(VCL-co-SBMA) hydrogels at 4, 25, 37 and 60°C; (B) Schematic illustration of the temperature dependence of P(VCL-co-SBMA) hydrogels and (C) Swelling and deswelling behaviors of hydrogel under heating-cooling cycles between 4 and 37°C.

The temperature-dependent ESR of P(VCL-co-SBMA) hydrogels are affected by the ratio of PVCL to PSBMA segments. At 4°C, the ESR gradually decreases with the increase of PSBMA segment (Figure 5A). The P(VCL-co-SBMA)$_1$ hydrogels show slightly less temperature sensitivity than that of the PVCL hydrogels, while the ESR of P(VCL-co-SBMA)$_2$ and P(VCL-co-SBMA)$_3$ hydrogels maintains at near-constant values from 4 to 60°C (Figure 5A). This is possibly caused by the competition between the intramolecular hydrophobic interactions among caprolactam moieties of PVCL segments and inter- and/or intra- electrostatic interactions among sulfobetaine groups of PSBMA segments (Figure 5B).[19] In addition, increase of PSBMA segments will enlarge the distance among caprolactam moieties of PVCL segments, resulting in the decrease of hydrogen bonding and hydrophobic interactions. Therefore, the temperature sensitivity of hydrogels decreases with the increase of PSBMA segments.

The reversible swelling behaviors were also studied at temperatures repetitive switched between 4°C and 37°C. As shown in Figure 5C, the ESRs of PVCL, PSBMA and P(VCL-co-SBMA)$_1$ hydrogels show reversible response to temperature switch cycles, while the ESRs of P(VCL-co-SBMA)$_2$ and P(VCL-co-SBMA)$_3$ hydrogels nearly remain constant in thermal cycles.

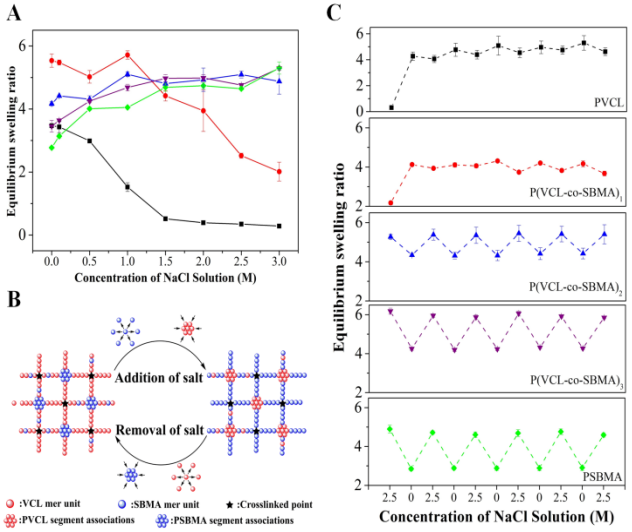

Figure 6. (A) Equilibrium swelling ratio of PVCL (■), P(VCL-co-SBMA)$_1$ (●), P(VCL-co-SBMA)$_2$ (▲), P(VCL-co-SBMA)$_3$ (▼), PSBMA (♦) hydrogels in NaCl solution with different ionic strength at 37°C; (B) Schematic illustration of the ionic strength dependence of P(VCL-co-SBMA) hydrogels; (C) Swelling and deswelling behavior of hydrogels in ionic strength cycles between 2.5 M NaCl solution and water.

3.5 Ion strength sensitivity of hydrogels

The ESRs of P(VCL-co-SBMA) hydrogels were also measured in the solution with the concentration of NaCl ranging from 0.1 to 3.0 M. As shown in Figure 6A, the ESR of PVCL hydrogel decreases in proportion with the increase of salt concentration, which can be explained by the "salting-out" effect around caprolactam moieties. The PVCL segments are collapsed in high concentration salt solutions, which can cause the osmotic pressure decrease and thus inhibit the hydration of the hydrogel.[39] In contrast, the ESR of PSBMA hydrogel shows incremental increase over the increase of NaCl concentration due to the effect of anti-polyelectrolyte around zwitterionic moieties. The Na^+ and Cl^- can shield the net attractive electrostatic interactions of ionic pairings of opposite charges between zwitterionic groups, and further cause the polymer chain expansion and thus enhance the hydration of the hydrogel. For P(VCL-co-SBMA) hydrogels, their swelling behavior in salt solutions depends on the competitive contribution of intramolecular hydrophobic interactions by PVCL segments and inter and/or intramolecular electrostatic interactions by PSBMA segments. For example, the "salting-out" effect is stronger than the anti-polyelectrolyte effect in P(VCL-co-SBMA)$_1$ hydrogel due to high ratio of PVCL segments, thus it shows similar swelling behavior with that of

PVCL hydrogels. Likewise, the P(VCL-co-SBMA)$_2$ and P(VCL-co-SBMA)$_3$ hydrogels that have high contents of PSBMA segments, display similar swelling behavior with that of PSBMA hydrogels due to the stronger anti-polyelectrolyte effect around PSBMA segments (Figure 6B).

We then tested the reversibility of swelling properties of P(VCL-co-SBMA) hydrogels in various salt concentrations. All hydrogels were subjected to cyclic water and 2.5 M NaCl solution and the corresponding ESRs were measured. As shown in Figure 6C, the P(VCL-co-SBMA)$_2$, P(VCL-co-SBMA)$_3$ and PSBMA hydrogels show reversible swelling behavior under salt switch cycles. However, the reversibility of P(VCL-co-SBMA)$_1$ and PVCL hydrogel is poor. The data suggest that PSBMA segments are mainly responsible for the salt-dependent reversible swelling behavior. However, it seems there are some discrepancies between the ESRs of ionic strength test and swelling/deswelling behavior test (Figure 6A & C). When the dry hydrogel directly immersed in 2.5 M NaCl solution, it absorbs little water due to the "salting-out" effect (Figure 6A).[19] After transferring them into water, the interactions among the PVCL segment decrease and lots of water come into hydrogel network via hydrogen bonds. However, when this swollen PVCL hydrogel is removed to NaCl solution, it is difficult for the water molecules to release from hydrogel due to the strong hydrogen bonds interactions between water and PVCL, resulting in the reversibility decreases with the increase of ratio of PVCL segments in hydrogel (Figure 6C).

3.6 Protein resistance of hydrogel

Thermorsensitive polymer usually can undergo a large conformation transition upon temperature change, which determines their specificity to either adsorb proteins or to desorb the bound proteins. In this study, IgG was used as the model protein to evaluate the protein adsorption of P(VCL-co-SBMA) hydrogels at different temperature. As shown in Figure 7, ELISA plate suffers substantial protein fouling at 4, 37, or 60°C. This phenomenon is also observed on PVCL hydrogels at 37°C and 60°C, while protein adsorption of PVCL hydrogels at 4°C is significantly suppressed. Moreover, the PSBMA hydrogels show the highest protein resistance at all tested temperatures. It suggests that the anti-biofouling properties of hydrogel depend on their hydrophilicity. The hydrophilic PSBMA segments can tightly bind to water molecules either through hydrogen bonding or ionic salvation to from a hydration layer, which can act as the energetic barrier for non-specific protein adsorption. The protein adsorption behavior of P (VCL-co-SBMA) hydrogels also undergoes temperature-dependent transition. At the temperature (4°C) below LCST, few detectable protein adsorptions are found on all P(VCL-co-SBMA) hydrogels (Figure 7). These results indicate that the P(VCL-co-SBMA) hydrogels exhibit switchable anti-biofouling. This phenomenon can be explained by the additional interactions of exposed hydrophilic chains of PVCL with water molecules, which can further prevent non-specific protein adsorption (Figure 8). In contrast, at the temperature (60°C) over the LCST, the surfaces of hydrogels would undergo a large conformational change to embed the hydrophilic groups of PVCL, and thus become more hydrophobic, which will favour non-specific protein adsorption (Figures 7 and 8). As such, the anti-biofouling level of P(VCL-co-SBMA) hydrogels generally reduces with the increase of PVCL segments when the temperature is above LCST (Figure 7).

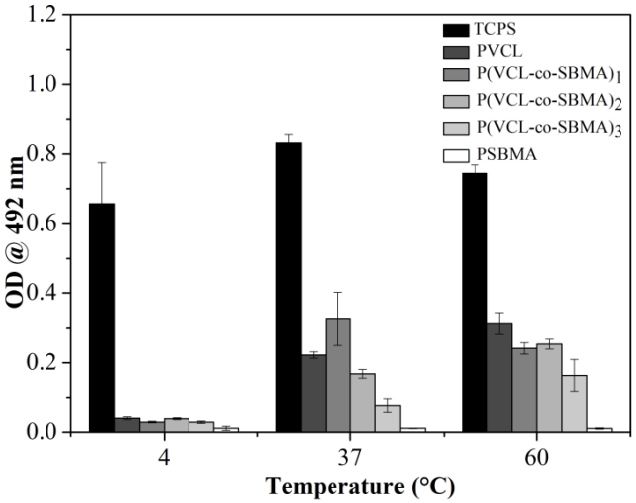

Figure 7. Adsorption behaviors of immunoglobulin G on the surfaces of PVCL hydrogel, P(VCL-co-SBMA) hydrogels, and PSBMA hydrogel at 4, 37 and 60°C in 0.1 M PBS.

3.7 Cell adhesion and proliferation

Cell adhesion is a typical assessment of the anti-biofouling ability of substrates.[45] The effects of hydrogel on cells adhesion were investigated via AO/PI staining. As shown in Figure 9, HUVECs adhere and spread into a confluent-like layer on the surface of TCPS and PVCL hydrogel at 37°C after 7 days. The introduction of PSBMA segments significantly reduces adhesion of HUVECs, as we find that the number of cells adhered on the hydrogel surface decreases along with the increase of PSBMA segments. In addition, few dead cells (red colour) are observed on all hydrogels surface (Figure 9), it indicates that these hydrogels have no cytotoxicity. The proliferation behavior of HUVECs on surface of hydrogel is evaluated by MTT assay. As shown in Figure 10, the cell viability of cells seeded on all P(VCL-co-SBMA) hydrogels decreases compared with that on PVCL hydrogels. Moreover, the proliferative capacity of HUVECs decreases with the increase of PSBMA segments in P(VCL-co-SBMA) hydrogel (Figure 10), indicating that the PSBMA segment is not beneficial for the cell proliferation. These phenomena might be caused by the following reasons: (i) Hydration of polymer chain may cause shielding of the hydrophobic groups and thus prevent the interactions of integrin of the cell with the hydrogel; (ii) cell spreading on hydrogels normally involves non-specific interaction of membrane proteins with the hydrogel surface. The protein resistance nature of PSBMA segment inhibits cell spreading.[18, 46, 47]

In order to evaluate the effect of temperature sensitivity on the cell detachment, cell detachment was evaluated as the temperature decreased from 37°C to 25°C or 4°C. It was observed that TCPS surface keeps its cell adhesion without any detachment at 4 and 25 °C within 120 min (Figure 11 and Figure S2), while the number of HUVECs attached on the surface of PVCL and P(VCL-co-SBMA)$_1$ hydrogel gradually decreases during the incubation period of 120 min at 4°C and 25°C. In addi-

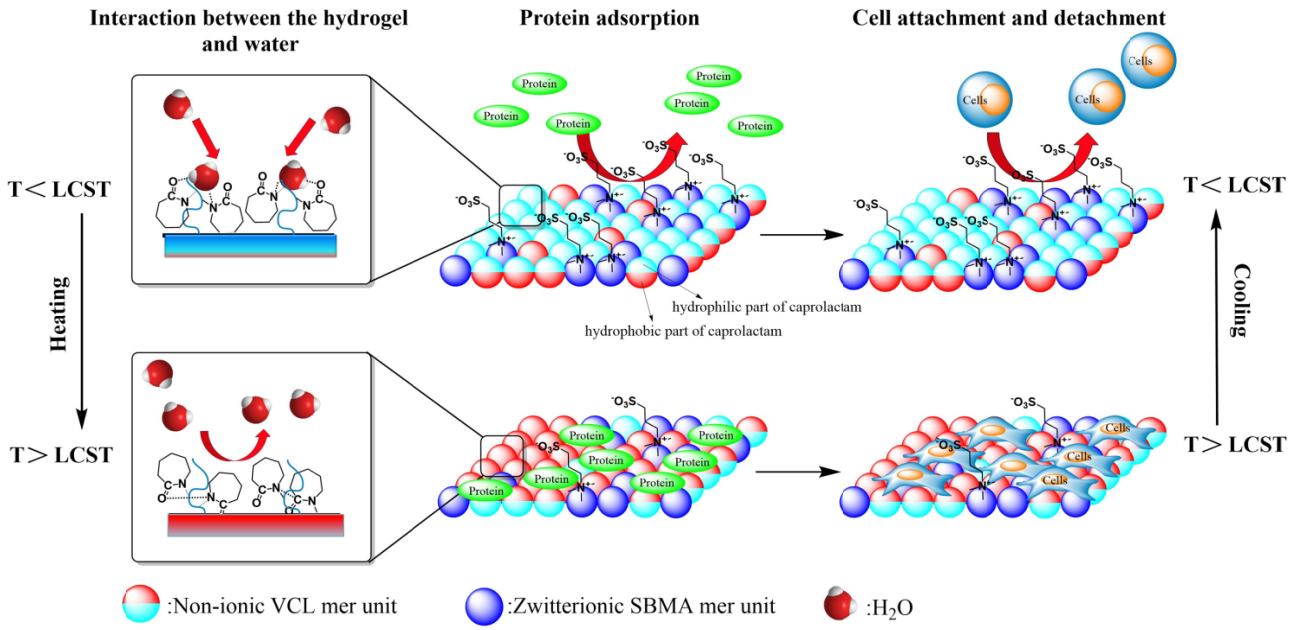

Figure 8. Schematic illustration of protein adsorption and cell attachment/detachment behaviors on P(VCL-co-SBMA) hydrogel surface.

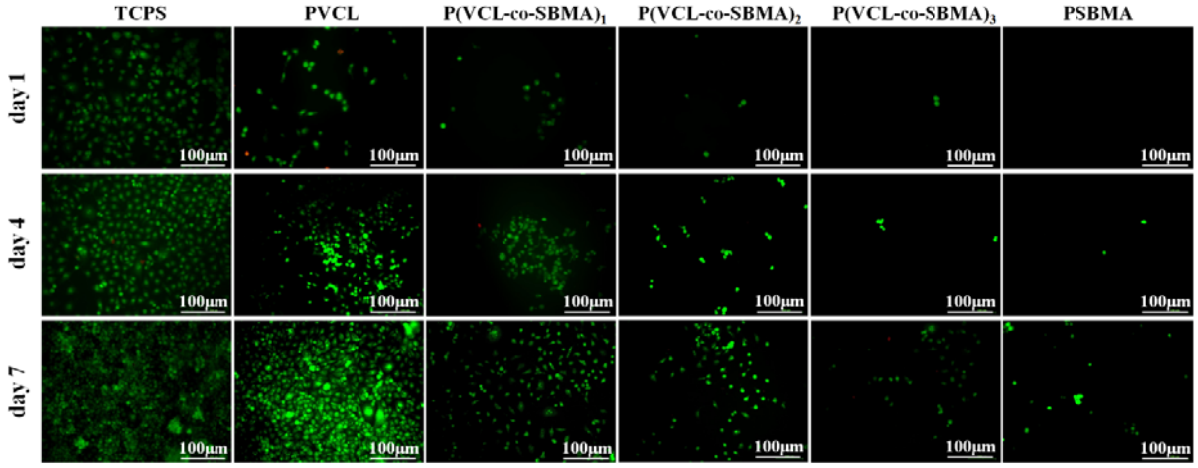

Figure 9. Fluorescence microscopic images of HUVECs cell seeded on P(VCL-co-SBMA) hydrogels cultured for 1, 4, and 7 days at 37°C.

-tion, the detachment capacity of HUVECs at 4°C is significantly higher than that at 25°C. Phase transition at different temperatures is the main factor to induce the HUVECs detaching from hydrogel surface. This result is correlated with the data of protein adsorption measurement presented above (Figure 7). When temperature is decreased, hydrophilic groups of PVCL segments may extend outward, resulting in cell detachment from the surface. In the case of P(VCL-co-SBMA)$_2$, P(VCL-co-SBMA)$_3$ and PSBMA hydrogel, the detachment of HUVECs is not obvious when the temperature decreases, because of only a small quantity of HUVECs can adhere on their surface due to the hydrophilic zwitterionic sulfobetaine groups which can strongly bind more water molecules (Figure 8). These results indicate that the P(VCL-co-SBMA) hydrogel can be used to control the attachment and detachment of cell.

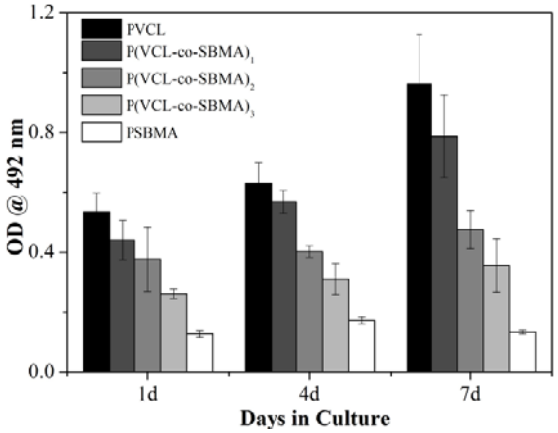

Figure 10. HUVECs proliferation behaviours seeded on P(VCL-co-SBMA) hydrogels within 7 days.

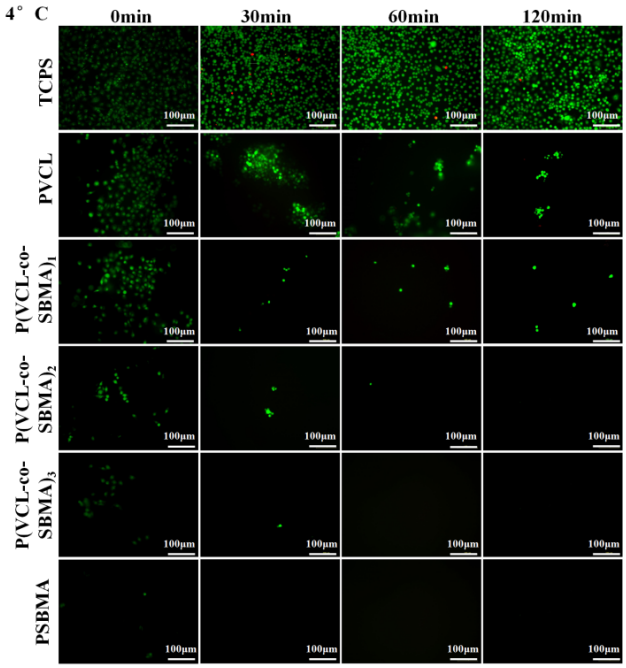

Figure 11. Fluorescence microscopic images of HUVECs detachment from the surfaces of TCPS, PVCL hydrogel, P(VCL-co-SBMA) hydrogels, and PSBMA hydrogel at 4°C for 0, 30, 60, and 120 min.

4. Conclusions

A series of P(VCL-co-SBMA) copolymer were successfully synthesized via homogenous reaction in water/DMSO media. These P(VCL-co-SBMA) copolymers can self-assemble into different types of aggregates in aqueous solution via adjusting temperature and ionic strength. P(VCL-co-SBMA) copolymers are soluble between UCST and LCST, and become insoluble beyond these temperatures. Moreover, with the increase of PSBMA segments in the copolymer chain, both LCST and UCST shift to higher temperatures. Furthermore, P(VCL-co-SBMA) hydrogels with cytocompatibility and switchable anti-biofouling were successfully prepared using MBAA as the cross-linker. Likewise, the copolymeric hydrogels exhibit good temperature sensitivity of the swelling performance and can be responsive to ion-strength stimuli owing to their PSBMA segments. In addition, they exhibit tunable protein resistance and cell adhesion via adjusting temperature and regulating the ratios of PVCL and PSBMA segments. At physiological temperature, the copolymeric hydrogels show excellent protein resistance. The attachment and proliferation capacity of HUVECs on the hydrogel surface decreases with the increase of PSBMA segments. Moreover, after 5 days cultured on the surface of our hydrogels, cells can easily detach from hydrogel with higher PVCL segments when the temperature decreases. In conclusion, our results demonstrate that the copolymeric hydrogel containing nonionic PVCL segments and zwitterionic PSBMA segments is a potential stimuli-responsive biomaterial providing switchable anti-biofouling.

Acknowledgment

This work is supported by National Nature Science Foundation of China (51073119, 31271016, 31370975, 31100674 and 81100782) and International Science & Technology Cooperation Program of China (No. 2013DFG30680).

Notes and references

[a] *School of Chemical Engineering and Technology, Tianjin University, Tianjin 300072, China. E-mail: yaofanglian@tju.edu.cn, Tel: +86-22-27402893 (Yao, F. L.);*
[b] *Department of Advanced Interdisciplinary Studies, Institute of Basic Medical Sciences and Tissue Engineering Research Center, Academy of Military Medical Science, Beijing 100850, China. Email: li41308@aliyun.com (Li, J. J.).*
[c] *Department of Chemistry and Biochemistry, University of Texas at Austin, 2500 Speedway, Austin, TX, 78712, USA*
[d] *Key Laboratory of Systems Bioengineering, Ministry of Education, Tianjin University, Tianjin 300072, China.*

†Electronic Supplementary Information: Preparation parameters of P(VCL-co-SBMA) hydrogels (Table S1); GPC traces of the copolymers (Figure S1); Fluorescence microscopic images of HUVECs cell detachment from the surfaces of the TCPS, the PVCL hydrogel, the P(VCL-co-SBMA) hydrogels, and the PSBMA hydrogel at 25°C for 0, 30, 60, and 120min (Figure S2); See DOI: 10.1039/b000000x/

1 Dimitrov, I.; Trzebicka, B.; Muller, A. H. E. Dworak A,Tsvetanov CB. *Prog. Polym. Sci.* 2007, **32**, 1275–1343.
2 Kharlampieva, E.; Pristinski, D.; Sukhishvili, S. A. *Macromolecules* 2007, **40**, 6967-6972.
3 Wang, Y.; Nie, J. S.; Chang, B. S.; Sun, Y. F.; Yang, W. L. *Biomacromolecules* 2013, **14**, 3034−3046.
4 Li, X.; Zhou, J.; Liu, Z.; Chen, J.; Lu, S.; Sun, H. *Biomaterials* 2014, **35**,5679-5688.
5 Purcell, B. P.; Lobb, D.; Charati, M. B.; Dorsey, S. M.; Wade, R. J.; Zellars, K. N. *Nat. Mater.* 2014, **13**, 653-661.
6 Shih, Y. J.; Chang, Y. *Langmuir* 2010, **26**, 17286-17294.
7 Lin, P.; Ding, L.; Lin, C. W.; Gu, F. *Langmuir* 2014, **30**, 6497-6507.
8 Kuo, W. H.; Wang, M. J.; Chien, H. W.; Wei, T. C.; Lee, C.; Tsai, W. B. *Biomacromolecules* 2011, **12**, 4348-4356.
9 Lalani, R.; Liu, L. *Biomacromolecules* 2012, **13**, 1853-1863.
10 Cao, Z. Q.;Jiang, S. Y. *Nano Today* 2012, **7**, 404-413.
11 Mi, L.; Xue, H.; Li, Y. T.; Jiang, S. Y. *Adv. Funct. Mater.* 2011, **21**, 4028–4034.
12 Wei, H.;Cheng, S. X.; Zhang, X. Z.; Zhuo, R. X. *Prog. Polym. Sci.* 2009, **34**, 893-910.
13 Liang, X.; Kozlovskaya, V.; Chen, Y.; Zavgorodnya, O.; Kharlampieva E. *Chem. Mater.* 2012**, 24**, 3707−3719.
14 Lee, B.; Jiao, A.; Yu, S.; You, J. B.; Kim, D. H.; Im, S. G. *Acta Biomater.* 2013**, 9**, 7691–7698.
15 Vihola, H.; Laukkanen, A.; Valtola, L.; Tenhu, H.;Hirvonen, J. *Biomaterials* 2005, **26**, 3055-3064.
16 Ramos, J.; Imazb, A.; Forcada, J. *Polym. Chem.* 2012, **3**, 852-856.
17 Chang, Y.; Shu, S. H.; Shih, Y. J.; Chu, C. W.; Ruaan, R. C.; Chen, W. Y. *Langmuir* 2010, **5**, 3522-3530.
18 Motoyasu, K.; Yuki T.; Moriya K.; Atsushi, T. *Soft matter* 2012, **29**, 11723-11731.
19 Chang, Y.; Yandi, W.; Chen, W. Y.; Shih, Y. J.; Yang, C. C.; Ling, Q. D. *Biomacromolecules* 2010, **11**, 1101-1110.
20 Chang, Y.; Chen, W. Y.; Yandi, W.; Shih, Y. J.; Chu, W. L.; Liu, Y. L. *Biomacromolecules* 2009**,10**,2092-2100.
21 Liu, L. D.; Wang, T.; Liu, C.; Lin, K.; Liu, G. M.; Zhang, G. Z. *J. Phys. Chem. B*. 2013, **117**, 10936-10943.
22 Dong, Z.; Mao, J.; Yang, M. Q.; Wang, D. P.; Bo, S. Q.; Ji, X. L. *Langmuir* 2011, **27**, 15282-15291.

23 Tian, M.; Wang, J. M.; Zhang, E. S.; Li, J. J.; Duan, C. M.; Yao, F. L. *Langmuir* 2013, **29**, 8076-8085.

24 Shao, Q.; Mi, L.; Han, X.; Bai, T.; Liu, S.; Li, Y. *J. Phys. Chem. B*. 2014, **118**, 6956-6962.

25 Shih, Y. J.; Chang, Y.; Deratani, A.; Quemener, D. *Biomacromolecules* 2012,**13**, 2849-2858.

26 Arotcüarena, M.; Heise, B.; Ishaya, S.; Laschewsky, A. *J. Am. Chem.Soc.* 2002, **124**, 3787-3793.

27 Lowe, S., O'Brien-Simpson, N. M, Connal, L. A. *Polym. Chem.* 2015, **6**, 198-122.

28 Li, M.; Neoh, K. G.; Xu, L. Q.; Wang, R.; Kang, E. T.; Lau, T. *Langmuir* 2012, **28**, 16408-16422.

29 Wang, J. M.; Sun, H.; Li, J. J.; Dong, D. Y.; Zhang, Y. B.; Yao, F. L. *Carbohyd. Polym.* 2015, **117**, 384-391.

30 Zhai, S. Y.; Ma, Y. H.; Chen, Y. Y.; Li, D.; Cao, J.; Liu, Y. J.; Cai, M. T.; Xie, X. X.; Chen, Y. M.; Luo, X. L. *Polym. Chem.* 2014, **5**, 1285–1297.

31 Zhao, Y.; Bai, T.;Shao, Q.; Jiang, S.; Shen, A. Q.; *Polym. Chem.* 2015, **6**, 1066-1077.

32 Zhang, Q.; Tang, X. D.; Wang, T. S.; Yu, F. Q.; Guo, W. J.; Pei, M. S. *RSC Adv.* 2014, **4**, 24240–24247.

33 Schilli, C. M.; Zhang, M. F.; Rizzardo, E.; Thang, S. H.; Chong, Y. K.; Edwards, K.; Karlsson, G.; Muller, A. H. E. *Macromolecules* 2004, **37**, 7861-7866.

34 Wan, D. H.; Zhou, Q.; Pu, H. T.; Yang, G. J. *J. Polym. Sci., Part A: Polym. Chem.* 2008, **46**, 3756-3765.

35 Singh, P.; Srivastava, A.; Kumar, R. *J. Polym. Sci., Part A: Polym. Chem.* 2012,**50**, 1503-1514.

36 Sun, S. T.; Wu, P. Y. *J. Phys. Chem. B.* 2011,**115**,11609-11618.

37 Cai, Y. L.; Tang, Y. Q.; Armes, S. P. *Macromolecules* 2004, **37**, 9728-9237.

38 Maeda, Y. S.; Nakamura, T.; Ikeda, I. *Macromolecules* 2002, **35**, 217-222.

39 Mikheeva, L. M.; Grinberg, N. V.; Mashkevich, A. Y.; Grinberg, Y. V. *Macromolecules* 1997, **30**, 2693-2699.

40 Deen, G. R.; Lim, E. K.; Mah, C. H.; Heng, K. M. *Ind. Eng. Chem. Res.* 2012, **51**, 13354-13365.

41 Liu, Q.; Patel, A. A.; Liu, L. *ACS. Appl. Mater. Interfaces.* 2014, **6**, 8996-9003.

42 Yang, M.; Liu, C.; Li, Z. Y.; Gao, G.; Liu, F. Q. *Macromolecules* 2010, **43**, 10645-10651.

43 Hashmi, S.; GhavamiNejad, A.; Obiweluozor, F. O.; Mohammad, V. V.; Stadler, F. J. *Macromolecules* 2012, **45**, 9804-9815.

44 Gao, Y. B.; Yeung, S. A.; Wu, C. *Macromolecules* 1999, **32**, 3674-3677.

45 Liu, P. S.; Chen, Q.; Li, L.; Lin, S. C.; Shen, J. *J. Mater. Chem. B,* 2014, **2**, 7222–7231

46 Chen, Y. S.; Tsou, P. C.; Lo, J. M.; Tsai, H. C.; Wang, Y. Z.; Hsiue, G. H. *Biomaterials* 2013, **34**, 7328-7334.